IEEE Access
Multidisciplinary | Rapid Review | Open Access Journal

Received July 6, 2021, accepted July 26, 2021, date of publication July 30, 2021, date of current version August 10, 2021.

Digital Object Identifier 10.1109/ACCESS.2021.3101413

An Optimal Higher Order Likelihood Distribution Based Approach for Strong Edge and High Contrast Restoration

LIANG ZHOU[1,2], ARVIND DHAKA[3], HASMAT MALIK[4], (Senior Member, IEEE), AMITA NANDAL[3], SATYENDRA SINGH[5], (Member, IEEE), AND TAO WU[1]

[1]Shanghai University of Medicine and Health Sciences, Shanghai 200240, China
[2]Center for Medicine Intelligent and Development, China Hospital Development Institute, Shanghai Jiao Tong University, Shanghai 200240, China
[3]Department of Computer and Communication Engineering, Manipal University Jaipur, Jaipur 303007, India
[4]Berkeley Education Alliance for Research in Singapore (BEARS), Research Center of the University of California, Berkeley, University Town, NUS Campus, Singapore 138602
[5]School of Electrical Skills, Bhartiya Skill Development University, Jaipur 302037, India

Corresponding authors: Hasmat Malik (hasmat.malik@gmail.com) and Amita Nandal (amita_nandal@yahoo.com)

This work was supported by the Foundation of National Key Research and Development Program of China under Grant 2020YFC2008700, in part by the National Natural Science Foundation of China under Grant 82072228 and Grant 92048205, in part by the Foundation of Shanghai Municipal Commission of Economy and Informatization under Grant 202001007, and in part by the three-year action plan for the Key Discipline Construction Project of Shanghai Public Health System Construction under Grant GWV-10.1XK05.

ABSTRACT The existing studies are generally focused on the pixel intensity or noise variance, and not much attention is given to describe the actual distribution. Some modifications have been proposed over the years in conventional parametric estimation techniques such as maximum likelihood estimation (MLE) and Bayesian estimation (BE). These methods have better properties to provide visually pleasing results for any imagery. In this paper, we use the likelihood estimate from the perspective that as the distribution order of likelihood increases, the overall effect of parameters under consideration improves within the defined confidence interval. In this paper, we use two parameters of interest, i.e., contrast and edge information. The proposed idea uses prior information w.r.t. particular parameter of interest, which is derived from likelihood estimate. The prior estimation has also been used to compute the reliability of the point estimations under a confidence interval. The proposed idea has desirable properties such that its optimization improves the overall image reconstruction.

INDEX TERMS Confidence interval, contrast parameter, edge detection, image priors, likelihood distribution orders, likelihood estimate, and image restoration.

I. INTRODUCTION

Parameter estimation techniques are used to estimate the parameters of a distribution model, which maximizes the fit to a particular data set. The most common methods used in mathematical statistics are maximum likelihood estimation (MLE) [1] and Bayesian estimation (BE) [2]. These techniques return the prior and posterior distribution of the parameters, where the mean of the posterior distribution is the best-fitting estimate of the parameters. A Bayesian framework interprets the obtained image as an accumulation of the original image [2]. For exponential families, the likelihood is a simple, standardized function of the parameters, and the conjugate priors are defined in the log-likelihood form. One of the significant drawbacks of parametric estimation techniques is resolution restoration. Therefore, image priors have been employed in various imaging applications to restore the image parameters efficiently. There are various statistical hypotheses that are supported by maximum likelihood estimation (MLE) [1], [3], [4]. MLE estimation is generally used for neighborhood smoothing. But, during neighborhood smoothing, the sharpness of edges may degrade. This paper addresses these issues by enhancing the contrast and edge sharpness of the image.

Generally, sparse signal representation is used in modern image processing techniques for linear and nonlinear

The associate editor coordinating the review of this manuscript and approving it for publication was Jiachen Yang.

transformations [5]. Most of the literature includes pixel intensity or noise variance, but their exact distribution is not defined. We have used statistical estimation of likelihood of image priors such that the contrast and edge information is restored. The priors use best-fitting parameters for accurate analysis of likelihood estimate [6], [7]. By simulating individual samples of the prior distribution, the actual parameter values can be recovered, which is assessed using the difference between first-order and second-order expected likelihood distribution. These estimates are then used to compute the reliability of the point estimations under a confidence interval.

In literature, various algorithms have been proposed for visual quality improvement of images. One of the basic algorithms is histogram equalization (HE) [8] which is widely used for contrast enhancement. There exist other variants of HE such as intensity-based mean-preserving HE, mean preserving sub histogram [9], [10]. One of the advantages of using mean preserving HE is that it reduces over enhancement but the degree of contrast enhancement is uncontrolled due to mean constraint. Therefore, we propose to maximize the likelihood estimate using the condition of the parameter of interest, and controlled estimation is carried out w.r.t. edge and contrast components.

Other researchers have considered optimization-based approaches for contrast enhancement [8], [9]. The optimization approaches provide flexibility for controlling different parameters for enhancement. In [11] and [12] authors have used intensity mapping function-based optimization for image enhancement. In [11], the authors used a mapping function-based optimization, which maximizes the signal variations for enhancement. In [12], the authors used a linear transformation-based optimization to restore the image structure for image enhancement. The aforementioned algorithms are extensively used for contrast enhancement, but they do not consider the statistical properties of images. However, in this paper we have evaluated the statistical estimation based on confidence interval to address these issues. In the proposed method, we have maximized the likelihood estimate based on edge and contrast component to improve the quality of the image.

The image priors provide better contrast between neighboring pixels. The different variants of priors have been extensively used in literature for image smoothing and contrast enhancement. The L1-norm and L2-norm is usually used in priors to analyze the effect of pixel-based luminance and interference caused in edge components. The total variation (TV) prior [13] uses the L1-norm of the gradient. Vector and Huber prior [14] use a combination of L1- and L2-norms. The Gaussian prior [2] analyses the effect of neighboring pixels as per Gaussian distribution. Generally, Markov random field (MRF) prior is used for edge restoration [15], [16]. The computation complexity of priors is typically high due to the exponential function usage. We try to improve the influence of likelihood order w.r.t. priors on the estimates in this paper.

Few researchers use posterior distribution estimation using maximum likelihood (ML) [1]. In this paper, the joint posterior distribution has been marginalized over the parameters of interest (edge, contrast) to determine exact value of the posterior mean. The choice of optimization method and parameter tuning is significant for exact estimation. In recent works for optimization, the variational expectation-maximization algorithm [15], variational Bayes approach [16], and majorization–minimization approach has been used. But, these methods affect image prior so that the accuracy of estimate reduces. In this paper, we propose to use an optimization problem so that the effect of edge and contrast enhancement is maximized.

We have compared our work with the existing prior models used for image enhancement. In [16], the Authors used a bilateral total variation (BTV) prior which is based on variational Bayesian analysis which enhances the visual quality of a low-resolution image. The drawback of this method is that the final image could not restore sharpness. This method has good noise suppression ability, but the results tend to be blurred. In [17], authors adopted the generalized Gaussian Markov field (GGMF) which is bound for heavy tail distributions. It is evident that in Heavy tails all moments may not exist, and few of the pixel information might be lost. This is overcome by computing higher-order statistics, which leads to increased computational complexity. In [18], the authors propose a heavy-tailed prior (HTP) based model which performs maximum a posteriori estimation for image enhancement. But, in these models, authors have focused on resolution enhancement only.

This paper is organized as follows; Section 2 provides the extraction of contrast and edge components. Section 3 details the proposed method. Image priors for enhancement are evaluated in Section 4. Section 5 presents modified likelihood coefficients. Optimization of likelihood distribution is presented in Section 6. Section 7 presents numerical results and discussion. Finally, Section 8 concludes the paper.

II. EXTRACTION OF CONTRAST AND EDGE COMPONENTS

The discrete image (I) of size $M \times N$ is given as matrix $I = [I_{ij}]$. The contrast matrix is $\mathbb{c} = \mathbb{c}(i,j)$ and edge matrix is $\mathbb{m} = \mathbb{m}(i,j)$ such that $i = 0, 1, 2, \ldots M-1$ and $j = 0, 1, 2, \ldots N-1$. The grayscale values of the discrete image lie in a range between 0 to 255. Clarity of an image can be significantly improved using contrast enhancement and edge detection methods [19, 20]. Extraction of such features from an image is one of the important issues [21]. We used the method presented in [22] to calculate the edge and contrast components of the image. Each edge component is the convolution between the image and its corresponding fractional differential pair [22]. The edge parameter ($\mathbb{m}$) corresponds to the magnitude of edge components such that

$$\mathbb{m}(i,j) = \frac{1}{\sqrt{\left(\mathcal{D}_x^{\alpha}\right)^2 + \left(D_y^{\alpha}\right)^2}} \left[\left\{ D_x^{\alpha} * I_{ij} \right\} + \left\{ D_y^{\alpha} * I_{ij} \right\} \right]. \quad (1)$$

Here, α is the order of Riemann-Liouville Fractional Derivative [21]. D_x^α and D_y^α are α order derivative of I_{ij} in x and y direction, respectively [22]. The contrast component ($\mathbb{c}$) is computed in reference to nearby pixels such that

$$\mathbb{c}(i,j) = \left(E_f(i,j) - E_b(i,j)\right) \times \ln\left[\frac{m_b(i-1,j-1)\,\overline{\ominus} m_f(i-1,j-1)}{m_b(i-1,j-1)\,\overline{\oplus} m_f(i-1,j-1)}\right]. \quad (2)$$

In eq. (2) the contrast component is computed in reference to nearby pixels to find relative values of these parameters with respect to one another. This is demonstrated by the pixel space $(i-1, j-1)$. $E_f(i,j)$ and $E_b(i,j)$ are foreground and background image entropy [22, 23]. $\overline{\ominus}$ and $\overline{\oplus}$ denote Logarithmic Image Processing (LIP) subtraction and addition respectively [24]. m_b and m_f denote mean gray value of background and foreground [24]. We set a threshold for $\mathbb{c}(i,j)$ such that we select only those pixels whose contrast is greater than a threshold ξ in the range from 0 to 1. We have computed the edges matrix using fractional calculus. Algorithm 1 presents the stepwise procedure to extract contrast and edge components.

Algorithm 1 Extraction of Contrast and Edge Components

1 **Input:** Input image, I_{ij}.
2 **Output:**Extraction of edge matrix ($\mathbb{m}(i,j)$) and contrast matrix ($\mathbb{c}(i,j)$).
3 Compute edge matrix, $\mathbb{m}(i,j)$ using directional derivatives of image I_{ij}.
4 Set a threshold ξ in the range from 0 to 1 so that in contrast matrix $\mathbb{c}(i,j)$ only those pixel values are stored whose contrast is greater than ξ.
5 Compute contrast matrix, $\mathbb{c}(i,j)$ with reference to nearby pixels in terms of foreground and background image entropy.
6 Return, edge matrix, $\mathbb{m}(i,j)$ and contrast matrix, $\mathbb{c}(i,j)$.

III. PROPOSED METHOD: FIRST ORDER LIKELIHOOD DISTRIBUTION

We first extract the contrast and edge matrices from the image and then their maximized likelihood estimates are computed. Later, we use an optimization method for maximization of statistical estimate. Figure 1 presents block diagram of the proposed methodology.

The likelihood function for $\mathbb{c}$ as contrast parameter and $\mathbb{m}$ as edge parameter is written as

$$\mathcal{L}(\mathbb{c},\mathbb{m}) = \prod_{\forall i,j}\left[\mathcal{L}(\mathbb{c})\,\mathcal{L}(\mathbb{m});\, I_{ij}\right]. \quad (3)$$

Here, I is an image vector of size $(M \times N)$. The likelihood w.r.t. contrast and edge parameter separately is written as

$$\mathcal{L}(\mathbb{c}) = \mathcal{L}\left(\mathbb{c}, \hat{\mathbb{m}}_{\mathbb{c}}; I_{ij}\right), \quad (4a)$$
$$\mathcal{L}(\mathbb{m}) = \mathcal{L}\left(\mathbb{m}, \hat{\mathbb{c}}_{\mathbb{m}}; I_{ij}\right). \quad (4b)$$

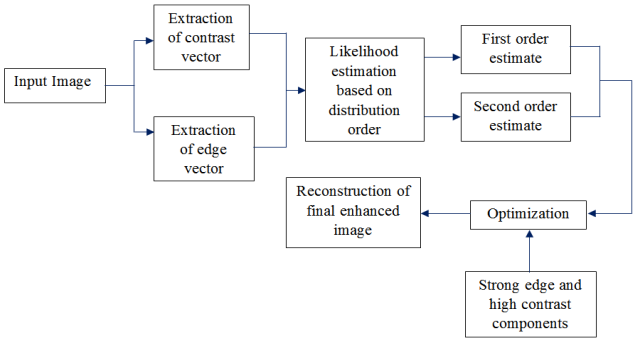

FIGURE 1. Block diagram showing proposed methodology.

$\hat{\mathbb{m}}_{\mathbb{c}}$ is the maximum likelihood estimate of $\mathbb{m}$ for fixed $\mathbb{c}$. $\hat{\mathbb{c}}_{\mathbb{m}}$ is the maximum likelihood estimate of $\mathbb{c}$ for fixed $\mathbb{m}$. Using Barndorff-Neilsen definition of the likelihood for first-order distribution [1] is written as

$$\mathcal{L}^1(\mathbb{c}) = \mathcal{L}(\mathbb{c})\,M(\mathbb{c}), \quad (5a)$$
$$\mathcal{L}^1(\mathbb{m}) = \mathcal{L}(\mathbb{m})\,M(\mathbb{m}). \quad (5b)$$

$M(\mathbb{c})$, $M(\mathbb{m})$ are first-order likelihood adjustment coefficients w.r.t. $\mathbb{c}$ and $\mathbb{m}$ respectively. When the value of contrast level is too low, then the estimate of $\mathcal{L}^1(\mathbb{c})$ is poor. When the value of edge strength level is too low, then the estimate of $\mathcal{L}^1(\mathbb{m})$ is poor. It can be improvised by choosing the proper values of the likelihood adjustment coefficient. In this paper, we use priors corresponding to the higher values of contrast component ($\mathbb{c}$), edge component ($\mathbb{m}$) by adjusting the level of likelihood coefficients i.e., $M(\mathbb{c})$ and $M(\mathbb{m})$ respectively. The values of $M(\mathbb{c})$ and $M(\mathbb{m})$ are computed using Fisher information form [25] such that

$$M(\mathbb{c}) = \frac{\left|f_{\mathbb{cc}}\left(\hat{\mathbb{c}}_{\mathbb{m}},\mathbb{m}\right)\right|^{\frac{1}{2}}\left|f_{\mathbb{cc}}\left(\hat{\mathbb{c}},\hat{\mathbb{m}}\right)\right|^{\frac{1}{2}}}{\left|l_{\mathbb{c};\hat{\mathbb{c}}}\left(\hat{\mathbb{c}}_{\mathbb{m}},\mathbb{m}\right)\right|}, \quad (6a)$$

$$M(\mathbb{m}) = = \frac{\left|f_{\mathbb{mm}}\left(\mathbb{c},\hat{\mathbb{m}}_{\mathbb{c}}\right)\right|^{\frac{1}{2}}\left|f_{\mathbb{mm}}\left(\hat{\mathbb{c}},\hat{\mathbb{m}}\right)\right|^{\frac{1}{2}}}{\left|l_{\mathbb{m};\hat{\mathbb{m}}}\left(\mathbb{c},\hat{\mathbb{m}}_{\mathbb{c}}\right)\right|}. \quad (6b)$$

where $l_{\mathbb{m};\hat{\mathbb{m}}}(\mathbb{c},\mathbb{m}) = \frac{\partial l(\mathbb{C},\mathbb{m})}{\partial \mathbb{C}\partial\hat{\mathbb{m}}^T}$ and $l_{\mathbb{c};\hat{\mathbb{c}}}(\mathbb{c},\mathbb{m}) = \frac{\partial l(\mathbb{c},\mathbb{m})}{\partial \mathbb{m}\partial\hat{\mathbb{c}}^T}$. $f_{\mathbb{mm}}(\mathbb{c},\mathbb{m})$ is the $\mathbb{mm}$-block of Fisher information of $f(\mathbb{c},\mathbb{m})$. $l(\mathbb{c},\mathbb{m}) = \log\mathcal{L}(\mathbb{c},\mathbb{m})$ is sample space derivative [25]. Algorithm 2 presents the stepwise procedure of first order likelihood estimation w.r.t. contrast and edge parameters.

IV. IMAGE PRIORS FOR ENHANCEMENT: EDGE AND CONTRAST PARAMETER BASED ESTIMATION

The possibility of adjusting likelihood functions $\mathcal{L}^1(\mathbb{c})$ and $\mathcal{L}^1(\mathbb{m})$ using priors [26], [27] helps to improve the image quality. The corresponding priors w.r.t $\mathbb{c}$ is written as

$$\mathcal{P}r(\mathbb{c}) \propto f_{\mathbb{cc.m}}\left(\hat{\mathbb{c}}_{\mathbb{m}},\mathbb{m}\right)^{\frac{1}{2}}. \quad (7)$$

$f_{\mathbb{cc.m}}\left(\hat{\mathbb{c}}_{\mathbb{m}},\mathbb{m}\right)$ is the Fisher information block, which is written as $f_{\mathbb{cc.m}}\left(\hat{\mathbb{c}}_{\mathbb{m}},\mathbb{m}\right) = f_{\mathbb{cc}}(\mathbb{c},\mathbb{m}) - f_{\mathbb{cm}}(\mathbb{c},\mathbb{m})\,f_{\mathbb{mm}}(\mathbb{c},\mathbb{m})^{-1}f_{\mathbb{mc}}(\mathbb{c},\mathbb{m})$.

Algorithm 2 First Order Likelihood Estimation w.r.t. Contrast and Edge Parameters

1 **Input:** Edge component $\mathbb{m}$ such that $\mathbb{m} = \mathbb{m}(i, j)$
Input: Contrast component $\mathbb{c}$ such that $\mathbb{c} = \mathbb{c}(i, j)$
2 **Output:** The first order likelihood adjustment coefficients i.e. $M(\mathbb{c})$, $M(\mathbb{m})$.
3 Calculate joint likelihood function ($\mathcal{L}(\mathbb{c}, \mathbb{m})$) for $\mathbb{c}$ as contrast parameter and $\mathbb{m}$ as edge parameter.
4 Calculate likelihood function w.r.t. contrast and edge parameter i.e. $\mathcal{L}(\mathbb{c})$ and $\mathcal{L}(\mathbb{m})$ respectively.
5 Compute likelihood coefficients, $M(\mathbb{c})$ and $M(\mathbb{m})$ using Fisher transformation.
6 Compute first order likelihood distribution using Barndorff-Neilsen w.r.t. contrast and edge parameter i.e. $\mathcal{L}^1(\mathbb{c})$ and $\mathcal{L}^1(\mathbb{m})$ respectively.
7. Return $M(\mathbb{c})$ and $M(\mathbb{m})$.
8. Return $\mathcal{L}^1(\mathbb{c})$ and $\mathcal{L}^1(\mathbb{m})$.

Algorithm 3 Image Priors Based Likelihood Estimation w.r.t. Edge and Contrast Parameters

1. **Input:** First order likelihood estimation w.r.t. contrast and edge parameter i.e. $\mathcal{L}^1(\mathbb{c})$ and $\mathcal{L}^1(\mathbb{m})$.
2. **Output:** Image priors based likelihood estimation i.e. $\mathcal{L}^{\mathcal{P}}(\mathbb{c})$ and $\mathcal{L}^{\mathcal{P}}(\mathbb{m})$.
3. Use Fisher transformation to compute Fisher information block w.r.t. edge and contrast components i.e. $f_{\mathbb{m}\mathbb{m}.\mathbb{c}}(\mathbb{c}, \hat{\mathbb{m}}_{\mathbb{c}})$ and $f_{\mathbb{c}\mathbb{c}.\mathbb{m}}(\hat{\mathbb{c}}_{\mathbb{m}}, \mathbb{m})$ respectively.
4. Compute likelihood function of strong priors w.r.t. contrast component i.e. $\mathcal{L}^{\mathcal{P}}(\mathbb{c})$.
5. Compute likelihood function of strong priors w.r.t. edge component i.e. $\mathcal{L}^{\mathcal{P}}(\mathbb{m})$.
6. Return, image priors based likelihood estimation w.r.t. contrast and edge components as $\mathcal{L}^{\mathcal{P}}(\mathbb{c})$ and $\mathcal{L}^{\mathcal{P}}(\mathbb{m})$.

$f_{\mathbb{c}\mathbb{c}}(\mathbb{c}, \mathbb{m})$, $f_{\mathbb{c}\mathbb{m}}(\mathbb{c}, \mathbb{m})$, $f_{\mathbb{m}\mathbb{m}}(\mathbb{c}, \mathbb{m})$ and $f_{\mathbb{m}\mathbb{c}}(\mathbb{c}, \mathbb{m})$ are the blocks of expected Fisher information from $\mathcal{L}^1(\mathbb{c}, \mathbb{m})$. For strong prior w.r.t. contrast component, the likelihood function now becomes,

$$\mathcal{L}^{\mathcal{P}}(\mathbb{c}) = \mathcal{L}^1(\mathbb{c}) f_{\mathbb{c}\mathbb{c}.\mathbb{m}}(\mathbb{c}, \hat{\mathbb{m}}_{\mathbb{c}}). \tag{8}$$

$\mathcal{L}^{\mathcal{P}}(\mathbb{c})$ contains better contrast information as compared to $\mathcal{L}^1(\mathbb{c})$. The corresponding prior w.r.t $\mathbb{m}$ is written as

$$\mathcal{P}r(\mathbb{m}) \propto f_{\mathbb{m}\mathbb{m}.\mathbb{c}}(\mathbb{c}, \hat{\mathbb{m}}_{\mathbb{c}})^{\frac{1}{2}}. \tag{9}$$

$f_{\mathbb{m}\mathbb{m}.\mathbb{c}}(\mathbb{c}, \hat{\mathbb{m}}_{\mathbb{c}})$ is the Fisher information block, which is written as $f_{\mathbb{m}\mathbb{m}.\mathbb{c}}(\mathbb{c}, \hat{\mathbb{m}}_{\mathbb{c}}) = f_{\mathbb{m}\mathbb{m}}(\mathbb{c}, \mathbb{m}) - f_{\mathbb{c}\mathbb{m}}(\mathbb{c}, \mathbb{m}) f_{\mathbb{c}\mathbb{c}}(\mathbb{c}, \mathbb{m})^{-1} f_{\mathbb{m}\mathbb{c}}(\mathbb{c}, \mathbb{m})$. $f_{\mathbb{c}\mathbb{c}}(\mathbb{c}, \mathbb{m})$, $f_{\mathbb{c}\mathbb{m}}(\mathbb{c}, \mathbb{m})$, $f_{\mathbb{m}\mathbb{m}}(\mathbb{c}, \mathbb{m})$ and $f_{\mathbb{m}\mathbb{c}}(\mathbb{c}, \mathbb{m})$ are the blocks of expected Fisher information from $\mathcal{L}^1(\mathbb{c}, \mathbb{m})$. For strong prior w.r.t. edge component, the likelihood function now becomes,

$$\mathcal{L}^{\mathcal{P}}(\mathbb{m}) = \mathcal{L}^1(\mathbb{m}) f_{\mathbb{m}\mathbb{m}.\mathbb{c}}(\hat{\mathbb{c}}_{\mathbb{m}}, \mathbb{m}). \tag{10}$$

$\mathcal{L}^{\mathcal{P}}(\mathbb{m})$ contains strong edge information as compared to $\mathcal{L}^1(\mathbb{m})$. The maximizer of eq. (8) and eq. (10) is a solution to an estimating equation obtained from higher-order distribution for parameters $\mathbb{c}$ and $\mathbb{m}$ which is detailed in the subsequent section. Therefore, an improvement is observed in the maximum likelihood estimator w.r.t. $\hat{\mathbb{c}}$ and $\hat{\mathbb{m}}$. $(\hat{\mathbb{c}}, \hat{\mathbb{m}})$ is maximum likelihood estimator of $(\mathbb{c}, \mathbb{m})$. Algorithm 3 presents the stepwise procedure of computing image priors based likelihood estimation w.r.t. edge and contrast parameters.

V. MODIFIED LIKELIHOOD COEFFICIENTS: SECOND ORDER LIKELIHOOD DISTRIBUTION

The likelihood adjustment coefficients also depend on the parameter $\mathbb{c}$ and $\mathbb{m}$ which is used to construct the distribution [6, 26] for $\mathbb{c}$ and $\mathbb{m}$. We present detailed steps to compute modified likelihood adjustment coefficient w.r.t $\mathbb{c}$ and later similar steps can be generalized w.r.t. $\mathbb{m}$. As we integrate the prior from eq. (7) over the parameter space the derivative of tail area approximation is obtained which follows Bayesian expansions [27]. It is written as

$$\int_{-\infty}^{\mathbb{c}} \mathcal{P}r(\mathbb{c})\, d\mathbb{c} = \phi\left(M^*(\mathbb{c})\right). \tag{11}$$

$\phi(.)$ is standard normal distribution function [7, 26]. $M^*(\mathbb{c})$ is the modified likelihood adjustment coefficient which is given as

$$M^*(\mathbb{c}) = M(\mathbb{c}) + \frac{1}{M(\mathbb{c})} \log \frac{q(\mathbb{c}, \mathbb{m})}{M(\mathbb{c})}, \tag{12}$$

$$q(\mathbb{c}, \mathbb{m}) = l'(\mathbb{c}, \mathbb{m}) \cdot \frac{\left|f_{\mathbb{c}\mathbb{c}.\mathbb{m}}(\hat{\mathbb{c}}, \hat{\mathbb{m}})\right|^{\frac{1}{2}}}{\left|f_{\mathbb{c}\mathbb{c}.\mathbb{m}}(\mathbb{c}, \hat{\mathbb{m}}_{\mathbb{c}})\right|^{\frac{1}{2}}} \cdot \frac{l_{\mathbb{m};\hat{\mathbb{m}}}(\mathbb{c}, \hat{\mathbb{m}}_{\mathbb{c}})}{\left|f_{\mathbb{m}\mathbb{m}}(\mathbb{c}, \hat{\mathbb{m}}_{\mathbb{c}})\right|^{\frac{1}{2}} \left|f_{\mathbb{m}\mathbb{m}}(\hat{\mathbb{c}}, \hat{\mathbb{m}})\right|^{\frac{1}{2}}}. \tag{13}$$

$l'(\mathbb{c}, \mathbb{m})$ is the derivative of $l(\mathbb{c}, \mathbb{m})$ w.r.t. $M^*(\mathbb{c})$ or $M^*(\mathbb{m})$ respectively. In view of this, the tail probability area the prior is the strong prior. More precisely, the value of first order likelihood ratio function can be used to derive a point estimate for $\mathbb{c}$ defined as a zero-level confidence interval. For values of $\mathbb{c}$, when $M^*(\mathbb{c}) = 0$ is the estimate of $\hat{\mathbb{c}}$ which improves the estimation. We follow similar steps to compute the modified likelihood adjustment coefficient w.r.t. $\mathbb{m}$ can be written as

$$M^*(\mathbb{m}) = M(\mathbb{m}) + \frac{1}{M(\mathbb{m})} \log \frac{q(\mathbb{c}, \mathbb{m})\, \mathcal{P}r(\mathbb{m})}{M(\mathbb{m})}. \tag{14}$$

Thus, the modified likelihood distribution w.r.t. $\mathbb{c}$ becomes

$$\mathcal{L}^2(\mathbb{c}) = -\frac{1}{2}\left(M^*(\mathbb{c})\right)^2 - \left[\log \mathcal{P}r(\mathbb{c}) + \log \frac{q(\mathbb{c}, \mathbb{m})\, \mathcal{P}r(\mathbb{c})}{M^*(\mathbb{c})}\right]. \tag{15}$$

Eq. (15) is a second-order equation. Eq. (15) shows that $\mathcal{L}^2(\mathbb{c})$ likelihood coefficient and prior ($\mathcal{P}r(\mathbb{c})$) can be

adjusted such that contrast information is preserved. Similarly, the modified likelihood distribution w.r.t. $\mathbb{m}$ becomes

$$\mathcal{L}^2(\mathbb{m}) = -\frac{1}{2}\left(M^*(\mathbb{m})\right)^2 - \left[\log \mathcal{P}r(\mathbb{m}) + \log \frac{q(\mathbb{c},\mathbb{m})\,\mathcal{P}r(\mathbb{m})}{M^*(\mathbb{m})}\right]. \tag{16}$$

If $\hat{\mathbb{c}}$ is maximizer of $\mathcal{L}^1(.)$ then it corresponds to $M(\mathbb{c})$. If $\hat{\mathbb{m}}$ is maximizer of $\mathcal{L}^1(.)$ then it corresponds to $M(\mathbb{m})$. Eq. (16) shows that $\mathcal{L}^2(\mathbb{m})$ likelihood coefficient and prior ($\mathcal{P}r(\mathbb{m})$) can be adjusted such that edge information is preserved. Algorithm 4 presents the stepwise procedure of computing modified likelihood as second-order likelihood distribution.

Algorithm 4 Computing Modified Likelihood as a Second Order Likelihood Distribution

1 **Input:** Fisher information block i.e. $f_{\mathbb{mm}.\mathbb{c}}(\mathbb{c}, \hat{\mathbb{m}}_{\mathbb{c}})$ and $f_{\mathbb{cc}.\mathbb{m}}(\hat{\mathbb{c}}_{\mathbb{m}}, \mathbb{m})$.
Input: First order likelihood adjustment coefficients i.e. $M(\mathbb{c})$, $M(\mathbb{m})$.
2 **Output:** Modified likelihood distribution w.r.t. contrast and edge parameter which takes the form of second-order likelihood i.e. $\mathcal{L}^2(\mathbb{c})$ and $\mathcal{L}^2(\mathbb{m})$ respectively.
3 Use first-order likelihood adjustment coefficients to compute modified likelihood adjustment coefficients w.r.t. contrast and edge parameter i.e. $M^*(\mathbb{c})$ and $M^*(\mathbb{m})$ respectively.
4 Use the likelihood ratio function for $\mathbb{c}$ and $\mathbb{m}$ to define confidence intervals.
5 Adjust the prior values w.r.t. contrast and edge component ($\mathcal{P}r(\mathbb{c})$ and $\mathcal{P}r(\mathbb{m})$ respectively) so that the contrast information and edge information are preserved.
6 Use the adjusted prior values from step 5 and modified likelihood coefficients from step 3 to compute $\mathcal{L}^2(\mathbb{c})$ and $\mathcal{L}^2(\mathbb{m})$.
7. Return, second-order likelihood i.e. $\mathcal{L}^2(\mathbb{c})$ and $\mathcal{L}^2(\mathbb{m})$.

VI. OPTIMIZATION OF LIKELIHOOD DISTRIBUTION AND FINAL IMAGE RECOVERY

We use the maximization problem for final image reconstruction. The likelihood distribution is further optimized using by maximization of I_{ij} w.r.t. $\mathbb{c}$ and $\mathbb{m}$. The transformed pixel vector can be represented using the maximization equation [28] as

$$\hat{I}(\mathbb{c},\mathbb{m}) = \frac{1}{\left(\mathcal{L}^2(\mathbb{c},\mathbb{m}) - \mathcal{L}^1(\mathbb{c},\mathbb{m})\right)^2}\|\mathbb{c},\mathbb{m}\|_2^2 + \lambda_1\left(\mathcal{L}^2(\mathbb{c},\mathbb{m})\right)^T \times \sum\nolimits_{\forall i,j}^{-1}\left(\mathcal{L}^2(\mathbb{c},\mathbb{m})\right) + \lambda_2\|\mathbb{c},\mathbb{m}\|_*. \tag{17}$$

$\hat{I}(\mathbb{c},\mathbb{m})$ is the contrast and edge maximized estimate of image I_{ij}. $\|.\|_*$ is the nuclear norm [29] of matrix $\mathbb{c}$ and $\mathbb{m}$. λ_1 and λ_2 are the weights of the likelihood and nuclear norm terms [29]. $\mathcal{L}^2(\mathbb{c},\mathbb{m}) - \mathcal{L}^1(\mathbb{c},\mathbb{m})$ is similar to statistical variance between first order and second order likelihood. We can maximize the overall objective function in eq. (17) by maximizing each term independently. To achieve this, we have used squared F-norm [29]. The I_{ij} is maximized w.r.t. $\mathbb{c}$ and $\mathbb{m}$ such that the overall effect of edges and contrast is maximized. The maximization equation is written as

$$\hat{I}(\mathbb{c},\mathbb{m}) = \underset{\mathbb{c},\mathbb{m}}{\operatorname{argmin}} \frac{1}{\left(\mathcal{L}^2(\mathbb{c},\mathbb{m}) - \mathcal{L}^1(\mathbb{c},\mathbb{m})\right)^2}\|\mathbb{c},\mathbb{m}\|_2^2 + \lambda_1\left(\mathcal{L}^2(\mathbb{c},\mathbb{m})\right)^T\sum\nolimits_{\forall i,j}^{-1}\left(\mathcal{L}^2(\mathbb{c},\mathbb{m})\right) + \left\|I_{ij} + [\mathbb{c},\mathbb{m}]\right\|_F^2 + \lambda_2\left\|I_{ij}\right\|_*. \tag{18}$$

Here, $\left\|I_{ij} + [\mathbb{c},\mathbb{m}]\right\|_F^2$ represents squared F-norm. $(\mathbb{c},\mathbb{m})$ represents the maximization of I_{ij} w.r.t. $\mathbb{c}$ and $\mathbb{m}$ such strong edges and high contrast components are extracted. In order to solve eq. (18) $\mathbb{c}$ is varied by keeping $\mathbb{m}$ fixed in I_{ij}. By doing this, the squared F-norm term becomes a quadratic function of $\mathbb{c}$. Therefore, the optimization w.r.t. $(\mathbb{c},\mathbb{m})$ in I_{ij} can be written as

$$\hat{I}(\mathbb{c},\mathbb{m}) = \underset{\mathbb{c},\mathbb{m}}{\operatorname{argmin}} \frac{1}{\left(\mathcal{L}^2(\mathbb{c},\mathbb{m}) - \mathcal{L}^1(\mathbb{c},\mathbb{m})\right)^2}\|\mathbb{c},\mathbb{m}\|_2^2 + \lambda_1\left(\mathcal{L}^2(\mathbb{c},\mathbb{m})\right)^T\sum_{\forall i,j}^{-1}\left(\mathcal{L}^2(\mathbb{c},\mathbb{m})\right) + \frac{\left\|I_{ij}[:,\mathbb{c}] + I_{ij}[:,\mathbb{m}] + [\mathbb{c},\mathbb{m}]\right\|_2^2}{(MN+1)\left(\mathcal{L}^2(\mathbb{c},\mathbb{m}) - \mathcal{L}^1(\mathbb{c},\mathbb{m})\right)^2}. \tag{19}$$

$\frac{1}{(MN+1)\left(\mathcal{L}^2(\mathbb{C},\mathbb{m}) - \mathcal{L}^1(\mathbb{C},\mathbb{m})\right)^2}$ is Lagrange multiplier [20] which is used to represented F-norm in form of squared norm. $I_{ij}[:,\mathbb{c}]$ represents the pixel vector with high contrast. $I_{ij}[:,\mathbb{m}]$ represents the pixel vector with strong edges. Since eq. (19) is quadratic in nature therefore, its derivative w.r.t. $\mathbb{c}$ and $\mathbb{m}$ will give eq. (20a) and eq. (20b) respectively. These are linear equations that can be written as

$$\left(\frac{MN+2}{MN+1} + \lambda, \left(\mathcal{L}^2(\mathbb{c},\mathbb{m}) - \mathcal{L}^1(\mathbb{c},\mathbb{m})\right)^2 . \sum\nolimits_{\forall i,j}^{-1}\mathcal{L}^2(\mathbb{c},\mathbb{m})\right)\mathbb{c} = \mathbb{c} + \lambda_1\left(\mathcal{L}^2(\mathbb{c},\mathbb{m}) - \mathcal{L}^1(\mathbb{c},\mathbb{m})\right)^2\sum\nolimits_{\forall i,j}^{-1}\mathcal{L}^2(\mathbb{c},\mathbb{m}) + \frac{I_{ij}[:,\mathbb{c}]}{MN+1}, \tag{20a}$$

$$\left(\frac{MN+2}{MN+1} + \lambda, \left(\mathcal{L}^2(\mathbb{c},\mathbb{m}) - \mathcal{L}^1(\mathbb{c},\mathbb{m})\right)^2 . \sum\nolimits_{\forall i,j}^{-1}\mathcal{L}^2(\mathbb{c},\mathbb{m})\right)\mathbb{m} = \mathbb{m} + \lambda_1\left(\mathcal{L}^2(\mathbb{c},\mathbb{m}) - \mathcal{L}^1(\mathbb{c},\mathbb{m})\right)^2\sum\nolimits_{\forall i,j}^{-1}\mathcal{L}^2(\mathbb{c},\mathbb{m}) + \frac{I_{ij}[:,\mathbb{m}]}{MN+1}. \tag{20b}$$

We can recover final image ($F(i,j)$) in pixel domain using strong edge and high contrast pixels only. The optimal solution of this maximization problem is

$$\mathcal{F}(i,j) = \underset{\mathbb{c},\mathbb{m}}{\operatorname{argmin}}\,\lambda_0\|\mathbb{c},\mathbb{m}\|_2^2 + \sum_{\forall i,j}\left\|I_{ij} + [\mathbb{c},\mathbb{m}]\right\|_F^2. \tag{21}$$

λ_0 is a positive constant [4]. Eq. (21) represents the final recovered image. Algorithm 5 presents the stepwise procedure of optimization of likelihood distribution and final image recovery.

Algorithm 5 Optimization of Likelihood Distribution and Final Image Recovery

1) [1] **Input:** $\mathcal{L}^1(\mathbb{c})$ and $\mathcal{L}^1(\mathbb{m})$ from algorithm 2. **Input:** $\mathcal{L}^2(\mathbb{c})$ and $\mathcal{L}^2(\mathbb{m})$ from algorithm 4.
2) [2] **Output:** Final optimized image, (F).
3) [3] Compute the statistical variance between first order and second order likelihood as $\mathcal{L}^2(\mathbb{c},\mathbb{m}) - \mathcal{L}^1(\mathbb{c},\mathbb{m})$.
4) [4] Compute transformed pixel vector using the maximization problem [26].
5) [5] Maximize the overall objective function of transformed pixel vector computed in step 4 w.r.t. $\mathbb{c}$ and $\mathbb{m}$ such that the overall effect of edges and contrast is maximized..
6) [6] Use squared F-norm w.r.t. $(\mathbb{c},\mathbb{m})$ for optimization of maximization function computed in Step 5.
7. Using F-norm in the form of squared norm compute contrast and edge optimized image vector as $I_{ij}[:,\mathbb{c}]$ (the pixel vector with high contrast) and $I_{ij}[:,\mathbb{m}]$ (the pixel vector with strong edges) respectively.
8. Recover final image $(\mathcal{F}(i,j))$ in pixel domain using strong edge and high contrast pixels as computed in step 7.
7) [9] Return, final optimized image, $\mathcal{F}(i,j)$.

VII. RESULTS AND DISCUSSION

This paper has shown various performance measures for comparison such as peak signal to noise ratio, entropy, structural similarity index measure, correlation coefficient, and local texture energy. In this paper, the image database from http://vision.middlebury.edu/stereo/data/ is used for evaluation [30]. We have used 18 reference images and presented the average numerical results. The input images are shown in Figure 2. The qualitative comparison among various methods is shown in Figure 3-5 for image size 128×128, 512×512 and 1024×1024 respectively. We have chosen contrast threshold as 0.4 for capturing the qualitative results for proposed method. However, the numerical results present the analysis by varying the contrast threshold as 0.8, 0.4 and 0.2 for proposed method.

Table 1 analyzes the likelihood deviation (d). It is observed that as deviation increases the efficiency of estimate improves. Mathematically, the deviation (d) are computed as $d = \left\|\left(\hat{\mathbb{c}},\hat{\mathbb{m}}\right) - (\mathbb{c},\mathbb{m})\right\|$. Here, $\left(\hat{\mathbb{c}},\hat{\mathbb{m}}\right)$ is maximum likelihood estimator of $(\mathbb{c},\mathbb{m})$. Table 1 summarizes the values of likelihood-based statistical estimate when the contrast threshold (ξ) is taken as 0.8, 0.4 and 0.2. This statistical estimate is observed for different image sizes as 1024×1024, 512×512 and 128×128. The image priors show dependency on image space therefore, when image size is changed, then the image specifics also change, which changes the final image appearance. Therefore, we have used a larger image size for better analysis. Most of the times the existing methods of finding the parameters of interest are unrealistic therefore, it is difficult to get exact estimate. In those cases, statistical estimate can used to make an estimate more accurate. From Table 1, we have observed the likelihood-based statistical estimate. The deviation is computed against each estimate. It is observed that when the deviation value is smaller when the image size is smaller and vice versa. Also, as deviation increases the efficiency of the estimate improves.

Table 2 gives empirical converges for equitailed 95% confidence interval of $M(\mathbb{c}), M(\mathbb{m})$ and $M^*(\mathbb{c}), M^*(\mathbb{m})$. The estimates are compared in terms of the parameters, which are relative to maximization of likelihood estimate respectively. A confidence interval provides more information about the parameter value in any estimate. Therefore, in this paper we have estimated the confidence interval w.r.t. edge and contrast parameters in the proposed likelihood distribution. When the probabilities converge faster in any confidence interval then it is concluded that the estimation is close to the nominal confidence level because the confidence interval observes the difference of the means of the normal distribution. In the proposed method, the confidence interval has observed the difference of the means w.r.t. contrast and edge parameters. It is also observed from Table 2 that the coverage probabilities under the confidence level of 0.95 are close to the nominal confidence level of 0.95 when the image sizes are large. From table 2 it can be noted that the maximizer of $\mathcal{L}^1(\mathbb{c},\mathbb{m})$ is preferable, which results in high contrast and strong edge restoration. This result is due to the fact that when this maximizer is computed w.r.t. $M^*(\mathbb{c})$ and $M^*(\mathbb{m})$ is based on second-order likelihood distribution. We illustrate that the proposed method improves the visual quality of image with the estimation of $\mathbb{c}$ and $\mathbb{m}$.

Table 3 examines the influence of likelihood order w.r.t. priors on the estimates. The use of priors in the likelihood estimation is considered as an objective statistical model. Any interference or noise in the input image and any change in size of input image is directly reflected in the uncertainty of priors. Therefore, in this paper our estimation is extended to different image sizes which allow us even to incorporate different features like edge and contrast. An advantage of a prior with reasonably small values of $\mathcal{L}^2(\mathbb{c},\mathbb{m}) - \mathcal{L}^1(\mathbb{c},\mathbb{m})$ is that the long tails truncate for the likelihood function. Therefore, we have to set the likelihood function in such a way that its distribution falls in center for given parameters in the data set. The likelihood, on the other hand, becomes more peaked with increasing image sizes and the area surrounding the peak is zero. It is observed that when prior takes a small value of likelihood variance $\left(\mathcal{L}^2(\mathbb{c},\mathbb{m}) - \mathcal{L}^1(\mathbb{c},\mathbb{m})\right)$, the peak is higher and vice versa.

In table 3 we have analyzed the variations in prior which is computed over the proposed estimation criteria. This variation in prior $\left(\mathcal{L}^2(\mathbb{c},\mathbb{m}) - \mathcal{L}^1(\mathbb{c},\mathbb{m})\right)$ is directly related to

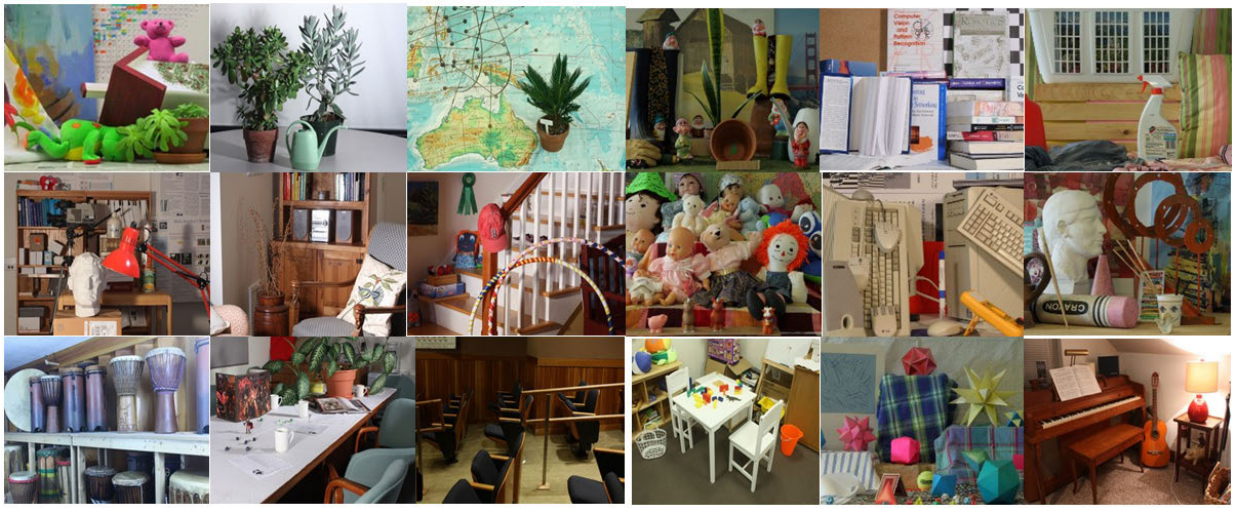

FIGURE 2. Input images Row 1: Image size 128 × 128, Row 2: Image size 512 × 512, Row 3: Image size 1024 × 1024.

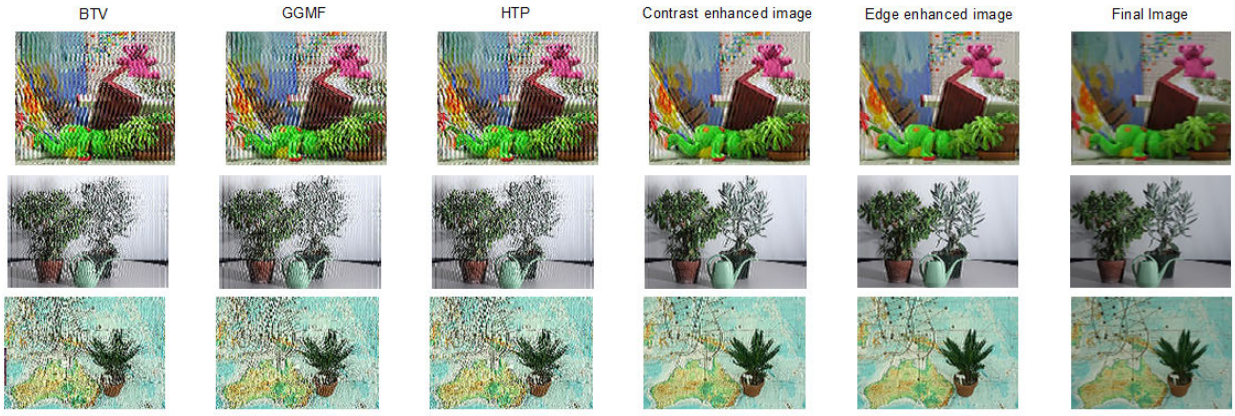

FIGURE 3. Qualitative comparison among various methods for input image size 128 × 128.

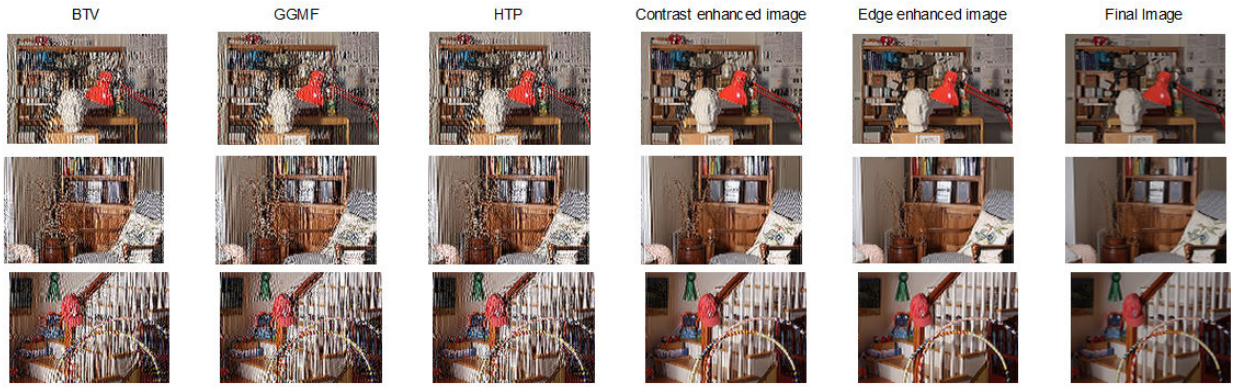

FIGURE 4. Qualitative comparison among various methods for input image size 512 × 512.

the probability measures using different parameter of interest used in this paper. This is a unique approach with respect to (w.r.t.) most of the works in literature, as we have targeted our choice of parameters of interest. This parameter is an important measure which reflects the uncertainty in the prior. Its small value indicates robustness. On the other hand, a large

FIGURE 5. Qualitative comparison among various methods for input image size 1024 × 1024.

FIGURE 6. Qualitative results for contrast and edge enhancement using proposed method for image size 128 × 128.

value is an indication that there is lack of robustness. It is observed from Table 3 that when the variation $\mathcal{L}^2(\mathbb{c}, \mathbb{m}) - \mathcal{L}^1(\mathbb{c}, \mathbb{m})$ is small then the value of PSNR is also reasonably good. A good set of priors should increase the precision of the estimates with a larger value of peak signal to noise ratio (PSNR). Peak signal to noise ratio (*PSNR*) is calculated as

$$PSNR = 20log_{10}\left(\frac{\mathcal{L}^2}{\frac{1}{MN}\sum_{i=0}^{M-1}\sum_{j=0}^{N-1}(I_{ij} - \hat{I}_{ij})^2}\right)$$

where $\mathcal{L}$ in the number of gray levels in the image. High PSNR value corresponds to a better reconstruction of the image.

A. CONTRAST COMPARISON METRIC

The good imaging method aims to restore contrast as best as possible. In this paper we present contrast comparison among original input and final output image by computing the difference between grey pixels and white pixels. We use contrast threshold (ξ) to separate the grey pixels and white pixels in image. Let us assume I^{in}_{grey} and I^{in}_{white} as average intensities of grey and white pixels in original input image respectively. We assume I^{out}_{grey} and I^{out}_{white} as average intensities of grey and white pixels in the final output image respectively. The contrast comparison metric (κ) is computed using the formula given in [31] such that $\kappa = \frac{I^{out}_{white}+I^{out}_{grey}}{I^{out}_{white}-I^{out}_{grey}} * \frac{I^{in}_{white}-I^{in}_{grey}}{I^{in}_{white}+I^{in}_{grey}}$. Fig. 9 shows contrast comparison among various methods w.r.t. SNR. It is observed from Fig. 9 that the performance of BTV and GGMF are very similar at both high and low SNRs, and the performance of the proposed method is best among them. However, for the proposed method, as SNR improves the contrast restoration capability improves as compared to conventional methods.

B. EDGE SHARPNESS METRIC

The image sharpness is measured by Tenengrad sharpness measure [32] using intensity values of pixels. The

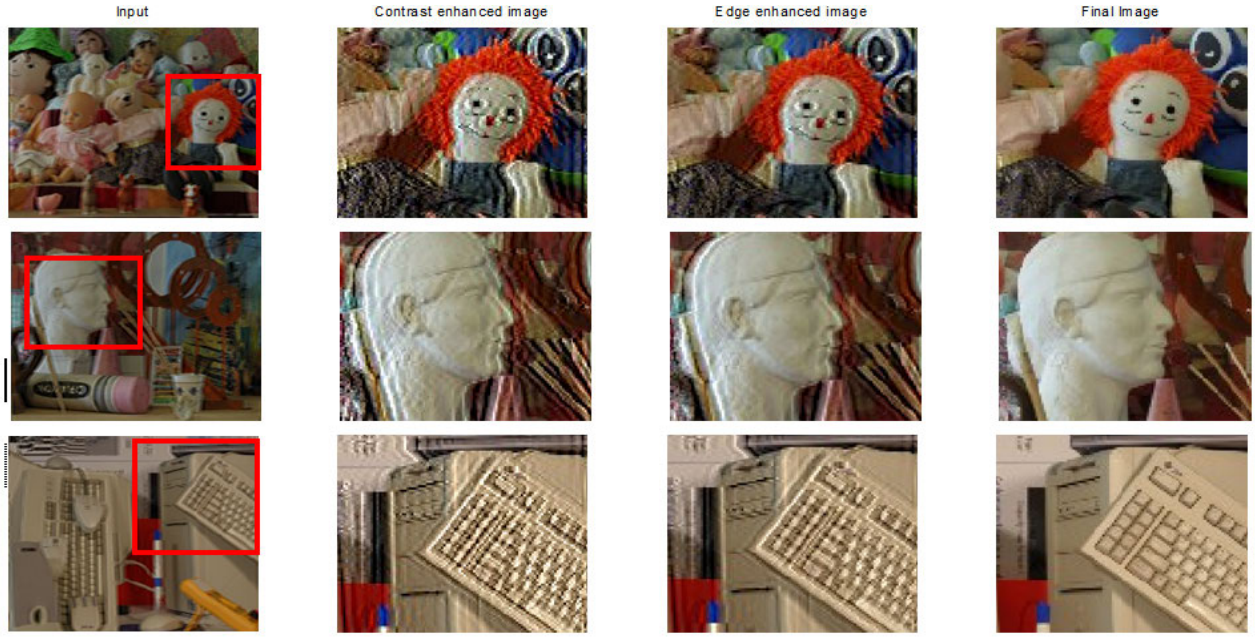

FIGURE 7. Qualitative results for contrast and edge enhancement using proposed method for image size 512 × 512.

FIGURE 8. Qualitative results for contrast and edge enhancement using proposed method for image size 1024 × 1024.

edge sharpness metric for original input image (s_{in}) is computed as $s_{in} = \sum_{\forall i}\sum_{\forall j}[I(i+1,j) - I(i-1,j)]^2 G_x^2 + [I(i,j+1) - I(i,j-1)]^2 G_y^2$. The edge sharpness metric for final output image (s_{out}) is computed as $s_{out} = \sum_{\forall i}\sum_{\forall j}[\mathcal{F}(i+1,j) - \mathcal{F}(i-1,j)]^2 G_x^2 + [\mathcal{F}(i,j+1) - \mathcal{F}(i,j-1)]^2 G_y^2$, where G_x and G_y are horizontal and vertical gradients computed using Sobel filter [33]. Sobel filter is capable of filtering more edges or make edges more visible as compared to other operator. This is because in sobel operator more weights are alotted to the pixel intensities around the edges. The Sobel method provides an approximation to the gradient magnitude and can even detect edges and their orientations. The overall edge sharpness metric ($\mathcal{S}$) difference between input and output image is given as $\mathcal{S} = \mathcal{S}_{out} - \mathcal{S}_{in}$. The sharpness metric is plotted for various methods in Fig. 10 It is observed from Fig. 10 that that the sharpness metric restores its value very slowly when SNR drops below 10dB for conventional methods. But for the proposed method the sharpness metric restoration is better than other methods. The restoration of the edge component deteriorates when external noise is introduced.

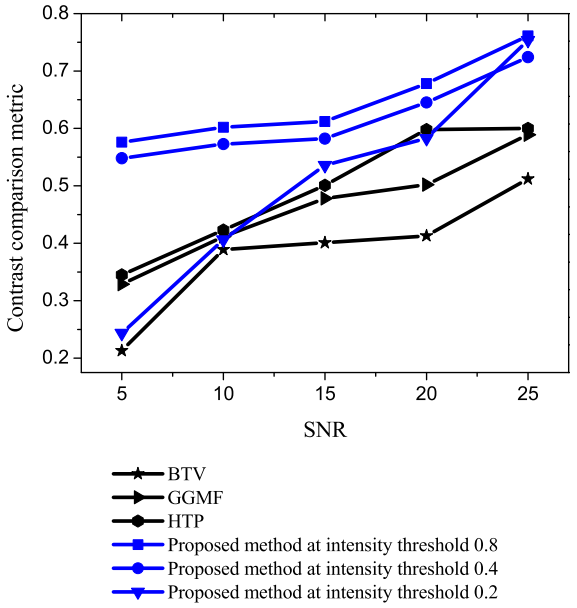

FIGURE 9. Plot showing contrast comparison metric w.r.t. SNR for various methods.

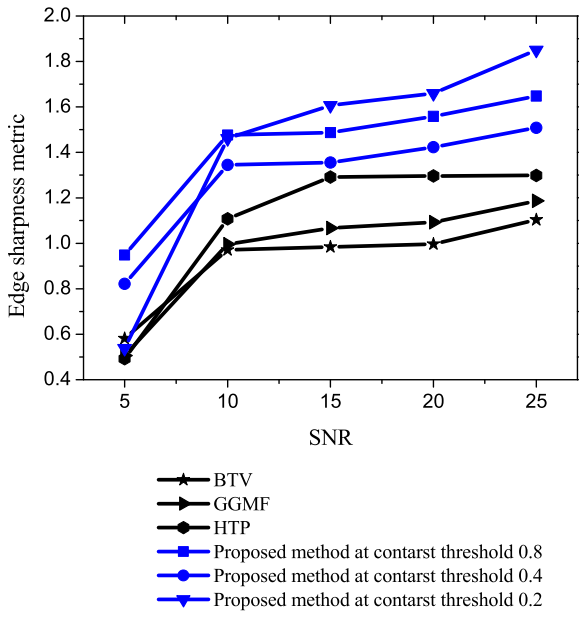

FIGURE 10. Plot showing edge sharpness metric w.r.t. SNR for various methods.

TABLE 1. Statistical estimate for proposed algorithm with average values from reference images.

	Statistical Estimate $(\mathbb{c}, \mathbb{m})$	$(\hat{\mathbb{c}}, \hat{\mathbb{m}})$	Deviation (d)
$\xi = 0.8$			
128×128	105.634	277.673	6.342
512×512	110.786	290.893	13.897
1024×1024	115.783	285.981	21.986
$\xi = 0.4$			
128×128	133.983	283.782	17.982
512×512	126.543	290.726	21.782
1024×1024	119.672	287.091	23.451
$\xi = 0.2$			
128×128	133.012	257.381	21.982
512×512	127.982	276.291	36.281
1024×1024	122.602	281.472	39.382

TABLE 2. Empirical converges of likelihood coefficients under 95% confidence interval with average values from reference images.

	128×128	512×512	1024×1024
$\xi = 0.8$			
$M(\mathbb{c})$	0.879	0.914	0.931
$M^*(\mathbb{c})$	0.937	0.932	0.946
$M(\mathbb{m})$	0.944	0.945	0.950
$M^*(\mathbb{m})$	0.966	0.951	0.952
$\xi = 0.4$			
$M(\mathbb{c})$	0.788	0.820	0.835
$M^*(\mathbb{c})$	0.840	0.836	0.849
$M(\mathbb{m})$	0.847	0.848	0.852
$M^*(\mathbb{m})$	0.867	0.853	0.854
$\xi = 0.2$			
$M(\mathbb{c})$	0.705	0.733	0.747
$M^*(\mathbb{c})$	0.752	0.748	0.759
$M(\mathbb{m})$	0.757	0.758	0.762
$M^*(\mathbb{m})$	0.775	0.763	0.764

TABLE 3. Variations in PSNR w.r.t. $\mathcal{L}^2(\mathbb{C}, \mathbb{m}) - \mathcal{L}^1(\mathbb{C}, \mathbb{m})$ with average values from reference images.

$\mathcal{L}^2(\mathbb{c}, \mathbb{m}) - \mathcal{L}^1(\mathbb{c}, \mathbb{m})$	0.01	0.02	0.04	0.05
$\xi = 0.8$				
128×128	21.021	21.654	20.503	20.237
512×512	22.298	21.628	20.639	20.211
1024×1024	22.461	21.500	20.248	18.995
$\xi = 0.4$				
128×128	13.083	13.344	11.411	11.256
512×512	13.129	12.956	10.553	10.649
1024×1024	13.813	13.750	12.345	10.474
$\xi = 0.2$				
128×128	11.678	11.397	8.716	6.619
512×512	12.485	11.359	9.969	8.690
1024×1024	12.636	10.132	9.148	8.136

In this paper for numerical analysis we have considered performance metrics like Entropy (E), Correlation coefficient ($\mathbb{C}$), Local texture energy (l), peak signal to noise ratio (PSNR) and structural similarity index measure (SSIM) [34-38]. Entropy (E) is the information content of image and it is represented as $E = -\sum_{i=0}^{\mathcal{L}-1} D_i log_2 D_i$. Here, $\mathcal{L}$ is the total of grey levels, $D_i = \{D_0, D_1, \ldots..D_{\mathcal{L}-1}\}$ is the probability distribution of each level [38].

The average correlation $\mathbb{C}$ can be expressed as

$$\mathbb{C} = \frac{F(i,j).I(i,j)}{\sqrt{\sum_{i=0}^{M-1}\sum_{j=0}^{N-1}(I\,(i,j)^2 + F(i,j)^2)}}. \tag{22}$$

The average correlation metric [37] provides quantitative measure of the degree of correlation.

TABLE 4. Comparison among various methods for different performance measures (Image size (128 × 128)).

Performance Metrics	State of art methods			Proposed method		
	BTV	GGMF	HTP	At ξ = 0.8	At ξ = 0.4	At ξ = 0.2
E	8.97	9.08	8.53	9.44	10.18	**11.7**
$\mathbb{C}$	0.73	0.71	0.74	0.73	0.79	**0.82**
ℓ	0.58	0.61	0.71	0.78	0.81	**0.89**
PSNR	18.34	19.97	18.53	**25.4**	22.33	21.67
SSIM	0.48	0.49	0.45	**0.7**	0.52	0.53

TABLE 5. Comparison among various methods for different performance measures (Image size (512 × 512)).

Performance Metrics	State of art methods			Proposed method		
	BTV	GGMF	HTP	At ξ = 0.8	At ξ = 0.4	At ξ = 0.2
E	11.08	10.28	9.66	10.7	11.53	13.25
$\mathbb{C}$	0.87	0.78	0.84	0.90	0.89	**0.93**
ℓ	0.68	0.71	0.74	0.81	**0.83**	0.81
PSNR	20.23	21.6	18.4	**25.69**	21.94	21.3
SSIM	0.45	0.5	0.58	**0.76**	0.48	0.54

Local texture energy (l) is an image quality assessment parameter that measures distortions affecting the image textures [34], [35]. We have used this metric to measure any impairment caused by contrast or edges. We have used this metric due to color images, because, texture and color have interdependent roles. We have used local binary patterns for analysing both color and texture information so as to predict the quality of images. Any noise or distortion in image decreases the local texture energy.

The local binary patterns operator incorporates color information separately, while keeping texture information restored [34]. We have computed the value of local texture energy using central pixel and the corresponding neighboring pixels as they have similar color channels. We have taken the value of neighboring pixels as 8 and analyzed its variation w.r.t. different image sizes to compare different algorithms. Mathematically, Local texture energy ($\mathcal{L}$) is computed as

$$\ell = \frac{\left(\sum_{p=0}^{\mathcal{P}-1} \mathcal{F}(i_{\mathbb{C}}, i_p).2^p\right).\mathcal{P} - \sum_{p=0}^{\mathcal{P}-1} \mathcal{F}(i_{\mathbb{C}}, i_p).\mathcal{D}}{\mathcal{P}^2}. \quad (23)$$

$$\mathcal{D} = \Delta\left(i_{p-1}, i_0\right) + \sum_{p=0}^{\mathcal{P}-1} \Delta\left(i_p, i_{p-1}\right) \quad (24a)$$

$$\Delta\left(.,.\right) = \mathcal{F}((i - i_{\mathbb{C}}), j) - \mathcal{F}(i, (j - i_{\mathbb{C}})) \quad (24b)$$

Here, $i_{\mathbb{C}}$ is center pixel, i_p is neighborhood pixel, $\mathcal{P}$ is number of neighbourhood pixel and $\mathcal{D}$ is deviation in the local texture energy w.r.t. neighborhood pixel. $\Delta\left(.,.\right)$ represents the variation function defined for pixel space in accordance to center pixel.

TABLE 6. Comparison among various methods for different performance measures (Image size (1024 × 1024)).

Performance Metrics	State of art methods			Proposed method		
	BTV	GGMF	HTP	At ξ = 0.8	At ξ = 0.4	At ξ = 0.2
E	11.36	11.49	10.8	11.96	12.89	**14.81**
$\mathbb{C}$	0.9	0.89	0.89	0.89	0.85	**0.97**
ℓ	0.69	0.76	0.75	**0.89**	0.87	0.88
PSNR	21.69	21.91	22.8	**26.33**	25.38	24.59
SSIM	0.51	0.59	0.73	**0.78**	0.56	0.65

Table 4, Table 5 and Table 6 show the comparison of different methods in terms of Entropy (E), Correlation coefficient ($\mathbb{C}$), Local texture energy (l), PSNR and SSIM for three different image sizes i.e. 128 × 128, 512 × 512 and 1024 × 1024 respectively. The image with high entropy has high information content. The image quality improves when $\mathbb{C}$ is closer to 1. If the value of l is close to unity then it is interpreted that the color texture restores well and it is assumed that distortions are less. On the other hand, if the l value deviates more from unity then there exist distortions in the image. The PSNR and SSIM are related to each other in such a way that when PSNR reduces, then the similarity between images also reduces and vice-versa. It is observed that PSNR and SSIM have the best values (in bold) using the proposed method. This is due to the fact if the long tails appear in the prior distribution, then the image quality degrades. It is also observed that for the larger image size the PSNR and SSIM take better values.

VIII. CONCLUSION

We propose an adjustment of likelihood distribution based on the parameters of interest. The proposed method corresponds to signal likelihood to follow second order distribution. The maximizer of proposed likelihood estimator improves image reconstruction. The numerical results present the observation related to the statistical estimate of likelihood distribution orders. As such, the prior no longer has any influence on the statistical estimates. However, in practical applications, it is not known if there is a critical sample size beyond which the prior has no influence anymore. Also, when the long tails of the likelihood function converge faster, the value of peak signal to noise ratio improves w.r.t. to different image sizes as analyzed in this paper.

ACKNOWLEDGMENT

This work was supported by the Foundation of National Key Research and Development Program of China under Grant 2020YFC2008700, in part by the National Natural Science Foundation of China under Grant 82072228 and Grant 92048205, in part by the Foundation of Shanghai Municipal Commission of Economy and Informatization under Grant 202001007, and in part by the three-year action plan for the Key Discipline Construction Project of Shanghai Public Health System Construction under Grant GWV-10.1XK05.

The authors would like to acknowledge the support from Intelligent Prognostic Private Limited Delhi, India Researchers Supporting Project, Intelligent Prognostic Private Limited Delhi, India.

REFERENCES

[1] O. Barndorff-Nielsen, "On a formula for the distribution of the maximum likelihood estimator," *Biometrika*, vol. 70, no. 2, pp. 343–365, 1983.
[2] M. E. Tipping and C. M. Bishop, "Bayesian image super-resolution," in *Advances in NIPS*. Cambridge, MA, USA: MIT Press, 2003, pp. 1279–1286.
[3] J. Peng, L. Li, and Y. Y. Tang, "Maximum likelihood estimation-based joint sparse representation for the classification of hyperspectral remote sensing images," *IEEE Trans. Neural Netw. Learn. Syst.*, vol. 30, no. 6, pp. 1790–1802, Jun. 2019.
[4] Y. Xu, S. Hu, and Y. Du, "Bias correction of multiple MRI images based on an improved nonparametric maximum likelihood method," *IEEE Access*, vol. 7, pp. 166762–166775, 2019.
[5] N. Bhalaji, K. B. Sundhara Kumar, and C. Selvaraj, "Empirical study of feature selection methods over classification algorithms," *Int. J. Intell. Syst. Technol. Appl.*, vol. 17, nos. 1–2, pp. 98–108, Jan. 2018.
[6] L. Pace and A. Salvan, "Adjustments of the profile likelihood from a new perspective," *J. Stat. Planning Inference*, vol. 136, no. 10, pp. 3554–3564, Oct. 2006.
[7] T. A. Severini, "Likelihood ratio statistics based on an integrated likelihood," *Biometrika*, vol. 97, no. 2, p. 116, Jun. 2010.
[8] Y.-T. Kim, "Contrast enhancement using brightness preserving bi-histogram equalization," *IEEE Trans. Consum. Electron.*, vol. 43, no. 1, pp. 1–8, Feb. 1997.
[9] Y. Wang, Q. Chen, and B. Zhang, "Image enhancement based on equal area qualistic subimage histogram equalization," *IEEE Trans. Consum. Electron.*, vol. 45, no. 1, pp. 68–75, Feb. 1999.
[10] S.-D. Chen and A. R. Ramli, "Contrast enhancement using recursive mean-separate histogram equalization for scalable brightness preservation," *IEEE Trans. Consum. Electron.*, vol. 49, no. 4, pp. 1301–1309, Nov. 2003.
[11] M.-S. Shyu and J.-J. Leou, "A genetic algorithm approach to color image enhancement," *Pattern Recognit.*, vol. 31, no. 7, pp. 871–880, Jul. 1998.
[12] Q. Shan, J. Jia, and M. S. Brown, "Globally optimized linear windowed tone mapping," *IEEE Trans. Vis. Comput. Graphics*, vol. 16, no. 4, pp. 663–675, Jul. 2010.
[13] S. Villena, M. Vega, S. D. Babacan, R. Molina, and A. K. Katsaggelos, "Image prior combination in super-resolution image registration & reconstruction," *Proc. IEEE Int. Workshop MLSP*, Nov. 2010, pp. 355–360.
[14] A. Kanemura, S. Maeda, and S. Ishii, "Hyperparameter estimation in Bayesian image superresolution with a compound Markov random field prior," in *Proc. IEEE Int. Workshop MLSP*, Aug. 2007, pp. 181–186.
[15] A. Kanemura, S.-I. Maeda, and S. Ishii, "Superresolution with compound Markov random fields via the variational EM algorithm," *Neural Netw.*, vol. 22, no. 7, pp. 1025–1034, 2009.
[16] S. D. Babacan, R. Molina, and A. K. Katsaggelos, "Variational Bayesian super resolution," *IEEE Trans. Image Process.*, vol. 20, no. 4, pp. 984–999, Apr. 2011.
[17] J. Chen, J. Nunez-Yanez, and A. Achim, "Video super-resolution using generalized Gaussian Markov random fields," *IEEE Signal Process. Lett.*, vol. 19, no. 2, pp. 63–66, Feb. 2012.
[18] J. Chen, J. L. Nunez-Yanez, and A. Achim, "Bayesian video super-resolution with heavy-tailed prior models," *IEEE Trans. Circuits Syst. Video Technol.*, vol. 24, no. 6, pp. 905–914, Jun. 2014.
[19] J. M. S. Prewitt, *Object Enhancement and Extraction, Picture processing and Psychopictorics*. New York, NY, USA: Academic, 1970, pp. 75–149.
[20] S. K. Maji, H. M. Yahia, and H. Badri, "Reconstructing an image from its edge representation," *Digit. Signal Process.*, vol. 23, no. 6, pp. 1867–1876, Dec. 2013.
[21] S. C. Agrawal, A. S. Jalal, and R. K. Tripathi, "Local and global features fusion to estimate expression invariant human age," *Int. J. Intell. Syst. Technol. Appl.*, vol. 19, no. 2, pp. 155–171, Apr. 2020.
[22] A. Nandal, H. Gamboa-Rosales, A. Dhaka, J. M. Celaya-Padilla, J. I. Galvan-Tejada, C. E. Galvan-Tejada, F. J. Martinez-Ruiz, and C. Guzman-Valdivia, "Image edge detection using fractional calculus with feature and contrast enhancement," *Circuits, Syst., Signal Process.*, vol. 37, no. 9, pp. 3946–3972, Sep. 2018, doi: 10.1007/s00034-018-0751-6.
[23] M. D. Ortigueira, *Fractional Calculus for Scientists and Engineers* (Lecture Notes in Electrical Engineering). Dordrecht, The Netherlands: Springer, 2011.
[24] M. Jourlin and J.-C. Pinoli, "Image dynamic range enhancement and stabilization in the context of the logarithmic image processing model," *Signal Process.*, vol. 41, no. 2, pp. 225–237, Jan. 1995.
[25] B. R. Frieden and R. A. Gatenby, *Exploratory Data Analysis Using Fisher Information*. London, U.K.: Springer, 2007.
[26] D. A. S. Fraser, "Likelihood for component parameters," *Biometrika*, vol. 90, no. 2, pp. 327–339, Jun. 2003.
[27] D. A. S. Fraser and N. Reid, "Strong matching of frequentist and Bayesian parametric inference," *J. Stat. Planning Inference*, vol. 103, nos. 1–2, pp. 263–285, Apr. 2002.
[28] W. R. Pestman and I. B. Alberink, *Mathematical Statistics: Problems and Detailed Solution*. Berlin, Germany: Walter De Gruyter, 1998.
[29] Z. Liu and L. Vandenberghe, "Interior-point method for nuclear norm approximation with application to system identification," *SIAM J. Matrix Anal. Appl.*, vol. 31, no. 3, pp. 1235–1256, 2009.
[30] *Online*. Accessed: Jan. 10, 2021. [Online]. Available: http://vision.middlebury.edu/stereo/data/
[31] R. D. Nowak, "Wavelet-based Rician noise removal for magnetic resonance imaging," *IEEE Trans. Image Process.*, vol. 8, no. 10, pp. 1408–1419, Oct. 1999.
[32] Y. Yao, B. Abidi, and M. Abidi, "Digital imaging with extreme zoom: System design and image restoration," in *Proc. 4th IEEE Int. Conf. Comput. Vis. Syst. (ICVS)*, Jan. 2006, p. 52.
[33] N. Kanopoulos, N. Vasanthavada, and R. L. Baker, "Design of an image edge detection filter using the Sobel operator," *IEEE J. Solid-State Circuits*, vol. 23, no. 2, pp. 358–367, Apr. 1988.
[34] P. Garcia Freitas, W. Y. L. Akamine, and M. C. Q. Farias, "Referenceless image quality assessment by saliency, color-texture energy, and gradient boosting machines," *J. Brazilian Comput. Soc.*, vol. 24, no. 1, pp. 1–6, Dec. 2018.
[35] O. A. Agudelo-Medina, H. D. Benitez-Restrepo, G. Vivone, and A. Bovik, "Perceptual quality assessment of pan-sharpened images," *Remote Sens.*, vol. 11, no. 7, p. 877, Apr. 2019.
[36] P. Gupta, Z. Sinno, J. L. Glover, N. G. Paulter, and A. C. Bovik, "Predicting detection performance on security X-ray images as a function of image quality," *IEEE Trans. Image Process.*, vol. 28, no. 7, pp. 3328–3342, Jul. 2019.
[37] G. Zhai and X. Min, "Perceptual image quality assessment: A survey," *Sci. China Inf. Sci.*, vol. 63, no. 11, Nov. 2020, Art. no. 211301.
[38] M. Selva, L. Santurri, and S. Baronti, "On the use of the expanded image in quality assessment of pansharpened images," *IEEE Geosci. Remote Sens. Lett.*, vol. 15, no. 2, pp. 320–324, Mar. 2018.

LIANG ZHOU is currently affiliated with Zhoupu hospital, Shanghai University of Medicine and Health Sciences, Shanghai, China. His main research interests include big data analysis and decision support.

ARVIND DHAKA received the Ph.D. degree in computer science and engineering from NIT Hamirpur, India (an institute of national importance), in 2018. Since 2018, he has been working as an Assistant Professor with the Department of Computer and Communication Engineering, Manipal University Jaipur. His research interests include wireless communication, wireless sensor networks, *ad-hoc* networks, medical image processing, machine learning, and deep learning in image processing.

HASMAT MALIK (Senior Member IEEE) received the M.Tech. degree in electrical engineering from the National Institute of Technology (NIT), Hamirpur, Himachal Pradesh, India, and the Ph.D. degree in electrical engineering from the Indian Institute of Technology (IIT), Delhi. He has served as an Assistant Professor for more than five years with the Division of Instrumentation and Control Engineering, Netaji Subhas Institute of Technology (NSIT), Dwarka, Delhi, India. He is currently a Chartered Engineer (C.Eng.) and a Professional Engineer (P.Eng.). He is also a Research Fellow with Berkeley Education Alliance for Research in Singapore (BEARS), Research Center of the University of California, Berkeley, University Town, National University of Singapore (NUS), Singapore, since January 2019. He has published widely in international journals and conferences his research findings related to intelligent data analytics, artificial intelligence, and machine learning applications in power systems, power apparatus, smart building and automation, smart grid, forecasting, prediction, and renewable energy sources. He has authored or coauthored more than 100 research articles and eight books and 13 chapters in nine other books, published by IEEE, Springer, and Elsevier. He has supervised 23 PG students. His research interests include artificial intelligence, machine learning, and big-data analytics for renewable energy, smart building and automation, condition monitoring, and online fault detection and diagnosis (FDD). He is also a member of the Computer Science Teachers Association (CSTA), the Association for Computing Machinery (ACM) EIG, the Institution of Engineering and Technology (IET), U.K., and MIR Labs, Asia, a Life Member of the Indian Society for Technical Education (ISTE), the Institution of Engineers (IEI), India, and the International Society for Research and Development (ISRD), London, and a fellow of the Institution of Electronics and Telecommunication Engineering (IETE). He received the POSOCO Power System Award (PPSA-2017) for his Ph.D. work for research and innovation in the area of power systems. He also received the Best Research Papers Awards from IEEE INDICON-2015 and the Full Registration Fee Award from IEEE SSD-2012, Germany.

AMITA NANDAL received the Ph.D. degree in electronics and communication engineering from SRM University, Chennai, in 2014. Since 2018, she has been working as an Associate Professor with the Department of Computer and Communication Engineering, Manipal University Jaipur. Her research interests include digital signal processing, machine learning and deep learning for medical image processing, wireless communication, circuits systems, and FPGA implementation.

SATYENDRA SINGH (Member IEEE) received the bachelor's (B.E.) degree in electrical engineering from the Government Engineering College Bikaner, Rajasthan, India, in 2008, the master's degree in power systems from the National Institute of Technology (NIT), Hamirpur, Himachal Pradesh, India, in 2011, and the Ph.D. degree in electrical engineering from the Malaviya National Institute of Technology (MNIT), Jaipur, India. He is currently working as an Assistant Professor with the School of Electrical Skills, Bhartiya Skill Development University, Jaipur, Rajasthan. His research interests include power systems, power system economics, electricity market, renewable energy modeling, facts devices, multi-agent systems, and nature-inspired algorithms.

TAO WU is currently affiliated with Shanghai University of Medicine and Health Sciences, Shanghai. His research interests include intelligent medicine and health management.